Open access • Journal Article • DOI:10.3171/JNS.1996.84.3.0449

Proton magnetic resonance spectroscopy in patients with glial tumors: a multicenter study — Source link

William G. Negendank, R. Sauter, Truman R. Brown, Jeffrey L. Evelhoch ...+15 more authors

Institutions: Fox Chase Cancer Center, Vita-Salute San Raffaele University

Published on: 01 Mar 1996 - Journal of Neurosurgery (Journal of Neurosurgery Publishing Group)

Topics: Glial tumor, In vivo magnetic resonance spectroscopy, Glioma and Astrocytoma

J Neurosurg 84:449–458, 1996

Proton magnetic resonance spectroscopy in patients with glial tumors: a multicenter study

WILLIAM G. NEGENDANK, M.D., ROLF SAUTER, PH.D., TRUMAN R. BROWN, PH.D., JEFFREY L. EVELHOCH, PH.D., ANDREA FALINI, M.D., EFSTATHIOS D. GOTSIS, PH.D., AREND HEERSCHAP, PH.D., KYOUSUKE KAMADA, M.D., BENJAMIN C. P. LEE, M.D., MICHEL M. MENGEOT, PH.D., EWALD MOSER, PH.D., KRISTIN A. PADAVIC-SHALLER, M.S.N., JOHN A. SANDERS, PH.D., THOMAS A. SPRAGGINS, PH.D., ARTHUR E. STILLMAN, M.D., PH.D., BURCKHARD TERWEY, M.D., THOMAS J. VOGL, M.D., KARSTEN WICKLOW, PH.D., AND ROBERT A. ZIMMERMAN, M.D.

Fox Chase Cancer Center, Philadelphia, Pennsylvania; Wayne State University, Detroit, Michigan; Mallinkrodt Institute, St. Louis, Missouri; Chicago Institute of Neurosurgery and Neuroresearch, Chicago, Illinois; University of New Mexico, Albuquerque, New Mexico; University of Virginia, Charlottesville, Virginia; University of Minnesota, Minneapolis, Minnesota; Children's Hospital of the University of Pennsylvania, Philadelphia, Pennsylvania; Siemens, AG, Erlangen; Saint Juergen Street Central Hospital, Bremen; and Free University, Berlin, Germany; San Raffaele Scientific Institute, Milan, Italy; Encephalos Institute, Halandri, Greece; University Hospital, Nijmegen, The Netherlands; Hokkaido University, Sapporo, Japan; and University of Vienna, Vienna, Austria

The authors represent a cooperative group of 15 institutions that examined the feasibility of using metabolic features observed *in vivo* with ^{1}H-magnetic resonance (MR) spectroscopy to characterize brain tumors of the glial type. The institutions provided blinded, centralized MR spectroscopy data processing along with independent central review of MR spectroscopy voxel placement, composition and contamination by brain, histopathological typing using current World Health Organization criteria, and clinical data. Proton ^{1}H-MR spectroscopy was performed using a spin-echo technique to obtain spectra from 8-cc voxels in the tumor and when feasible in the contralateral brain. Eighty-six cases were assessable, 41 of which had contralateral brain spectra. Glial tumors had significantly elevated intensities of choline signals, decreased intensities of creatine signals, and decreased intensities of *N*-acetylaspartate compared to brain. Choline signal intensities were highest in astrocytomas and anaplastic astrocytomas, and creatine signal intensities were lowest in glioblastomas. However, whether expressed relative to brain or as intratumoral ratios, these metabolic characteristics exhibited large variations within each subtype of glial tumor. The resulting overlaps precluded diagnostic accuracy in the distinction of low- and high-grade tumors. Although the extent of contamination of the ^{1}H-MR spectroscopy voxel by brain had a marked effect on metabolite concentrations and ratios, selection of cases with minimal contamination did not reduce these overlaps. Thus, each type and grade of tumor is a metabolically heterogeneous group. Lactate occurred infrequently and in all grades. Mobile lipids, on the other hand, occurred in 41% of high-grade tumors with higher mean amounts found in glioblastomas. This result, coupled with the recent demonstration that intratumoral mobile lipids correlate with microscopic tumor cell necrosis, leads to the hypothesis that mobile lipids observed *in vivo* in ^{1}H-MR spectroscopy may correlate independently with prognosis of individual patients.

KEY WORDS • brain neoplasm • glioma • magnetic resonance spectroscopy • lipids • metabolite

THE prognostic significance of histopathological and molecular biological factors in brain tumors is of interest because these factors are potentially able to guide clinical management decisions.[52] The association between poor survival of patients with glial tumors and glucose hypermetabolism determined by positron emission tomography (PET)[1,23,25,44,56] raised interest in examining correlations between visualizable *in vivo* metabolic features and prognosis in brain tumors. Recently, proton ^{1}H-nuclear magnetic resonance (NMR) spectroscopy has also been applied to study metabolic aspects of brain tumors. Nuclear magnetic resonance spectroscopy uses radiofrequency excitation in the presence of a magnetic field to obtain signals from naturally occurring ^{1}H nuclei to identify and quantitate metabolites. The most commonly acquired ^{1}H-NMR spectra of brain have three major peaks, one containing primarily signals from cholines (choline, phosphorylcholine, and glycerophospho-

rylcholine), one primarily from creatines (creatine and phosphocreatine), and one primarily from *N*-acetylaspartate (NAA). In disease, signals from lactate and mobile lipids may also be observed.

Studies of extracts of surgical specimens of human astrocytic tumors using ^{1}H-NMR spectroscopy indicated an increase in the ratio of cholines to creatines, and a decrease in the ratio of NAA to creatines, with increasing histopathological grades of malignancy.[16,45,61] Studies in patients using ^{1}H-NMR spectroscopy, referred to as MR spectroscopy, indicated similar correlations between metabolic features *in vivo* and the histopathological grades of astrocytic tumors.[4,11,14,21,32,43,57,58,61] Other MR spectroscopy studies indicated that lactate is more likely to be present in high- than in low-grade tumors[4,14,15,20,21] and that the amount of lactate may correlate with the extent of hypermetabolic glucose consumption shown in PET.[2,14,22] In a recent study, lipids were recognized *in vivo* in 23% of spectra from 48 gliomas and the authors suggested that these lipids occur with higher incidence in tumors of higher histopathological grade;[43] this agrees with the finding in intact surgical specimens that higher grade astrocytic tumors contain mobile lipids, the amounts of which correlate with the amount of microscopic cellular necrosis.[31]

In all published studies, metabolic signal intensities had large coefficients of variation within, and overlaps between, histopathological grades of glial tumors. Moreover, trends in metabolic changes among different grades were inconsistent. For example, in some studies the choline/creatine ratio did not progressively increase with increasing grade,[11,14,32] and in some the level of NAA did not progressively decrease with increasing grade but was higher in high grades than in intermediate ones or in intermediate grades compared to low ones.[4,11,32,43,57,61] The variations and overlaps have precluded diagnostic use of ^{1}H-MR spectroscopy to distinguish grades of glial tumors. Factors that may contribute to this and to different results from different studies include: nonuniformity of histopathological grading systems; spatial variations in grading within a tumor; nonuniformity of techniques used to localize ^{1}H-NMR spectra to the region of interest; and variable attempts to avoid contamination of spectra by metabolites from edematous brain and obvious nonviable regions of tumors. Different ^{1}H-MR spectroscopy acquisition parameters, in particular, different echo and repetition times, modulate metabolite signal intensities in different ways. Finally, the identification and quantitation of lipids *in vivo* requires methods that permit distinction between intratumoral lipids and contaminant lipid signals from the skull or scalp and between lipid and lactate signals that overlap one another.

To attempt to overcome some of these limitations, accrue a sizable number of patients with different grades of glial tumors in a short time, and define more accurately the potential of *in vivo* single-voxel ^{1}H-MR spectroscopy to characterize primary brain tumors, we organized a cooperative group consisting of 15 institutions using identical acquisition techniques in similar clinical instruments. Our study, preliminary accounts of which have been presented elsewhere,[39,40] provides blinded uniform MR spectroscopy data processing at a central location, uniform histopathological typing, uniform criteria for case selection, and quantitation of lipids and lactate.

Clinical Material and Methods

Establishment of the Cooperative Group and Technical Quality-Control Procedures

Institutional eligibility required: 1) a Siemens 1.5-tesla magnetic field–strength Magnetom SP with A2.3 software and a circularly polarized head coil; 2) a standard ^{1}H-MR spectroscopy protocol; and 3) the ability to meet quality-control criteria established in a preceding study. In the preceding study spectra were obtained using a spin-echo technique[7] from nominal 8-cc voxels in parietooccipital lobes and basal ganglia of six volunteers at each of 38 institutions.[53] Technical quality-control procedures performed on phantoms and volunteers included calibration of transmitter adjustment, global shimming to adjust for static B_o inhomogeneity, eddy current adjustments, local shimming to adjust for local static and dynamic B_o inhomogeneity, and calibration of water suppression. The first criterion for acceptance of MR spectroscopy data from an individual case included absence of any artifacts resulting from miscalibration or misadjustment of shimming, eddy-current correction, or water suppression, which interfere with analysis of metabolite intensities. The second criterion was an adequate signal-to-noise ratio to permit reproducible peak area integration. The third criterion, applicable to NMR spectra from voxels placed near the skull, was absence of contaminating lipid signals, which overlap or distort other peaks in the spectrum.

Patient Selection

Patients of any age with newly diagnosed or recurrent primary brain tumors of the glial subtype were examined. The initial criteria for inclusion in this study were: 1) acceptable quality of the spectrum; 2) evidence on MR imaging of a tumor occupying at least half the volume of the 8-cc MR spectroscopy voxel; and 3) histological confirmation of the diagnosis at some time in the course of the disease. We accepted recurrent cases if they had adequate objective clinical evidence of recurrence of tumor including rebiopsy and/or diagnostic MR imaging and computerized tomography scans. We included four cases with a clinical diagnosis of astrocytoma that was made without a biopsy because they had typical clinical and MR imaging features and a biopsy could have caused unnecessary brainstem damage.

Data Flow, Database, and Evaluation

Magnetic resonance imaging, histological, clinical, and demographic data were submitted to Fox Chase Cancer Center for central review. The algorithm by which cases were evaluated and included or excluded from analysis is summarized in Fig. 1.

Clinical MR imaging studies were required to meet the following criteria: 1) images had to be produced in at least two planes to permit accurate definition of the MR spectroscopy voxel placement; 2) images had to be sufficient to permit an independent outside observer to assess the presence of a solid, apparently viable tumor and the voxel

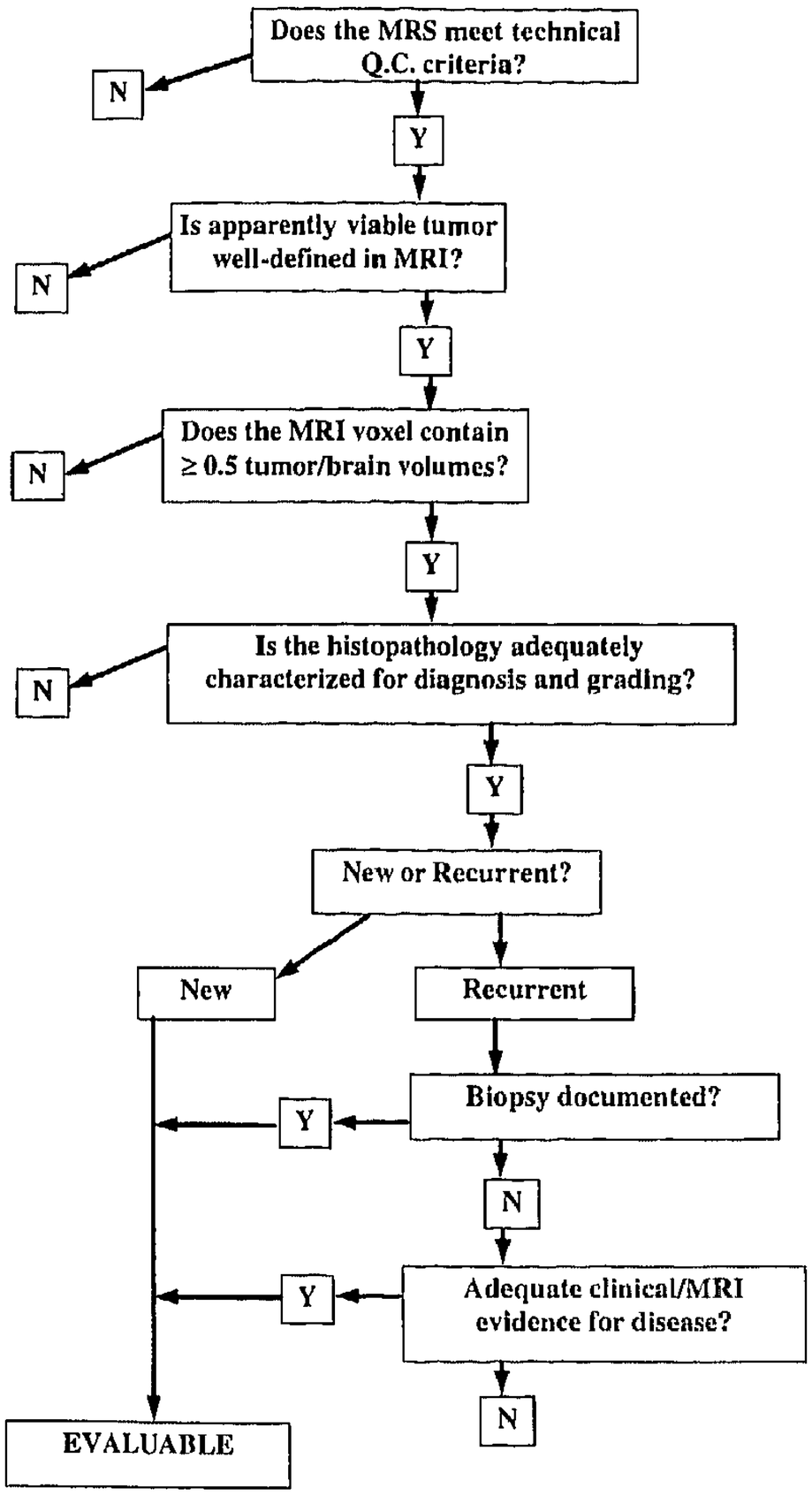

FIG. 1. Evaluation algorithm used in the study. MRI = magnetic resonance imaging; MRS = magnetic resonance spectroscopy; Q.C. = quality control.

placement relative to it; and 3) images had to be submitted for central review. The compositions of the MR spectroscopy voxels were assessed independently using all available MR imaging studies and expressed as fractions of solid tumor, edematous brain, nonedematous brain, liquefaction necrosis, cystic hemorrhagic necrosis, simple cysts, surgical cystic defects, ventricle, and extramedullary tissue (for example, skull). The region of solid tumor was often readily apparent in a combination of standard T_1- and T_2-weighted images. However, in accordance with recent experience,[19] we found that for many astrocytic tumors and for most tumors that recurred after prior treatment, contrast enhancement was necessary to define the location and extent of apparently viable tumor and to differentiate it from cystic necrosis and edematous brain. The ratio of the volume of solid tumor to that of solid tumor plus brain (tumor/tumor + brain) was calculated and is referred to as the "tumor fraction." In this expression, the term "tumor" is used only to describe solid tumor, not cystic or necrotic regions, and the term "brain" includes edematous and nonedematous brain. We accepted any case with an estimated tumor fraction in the 8-cc MR spectroscopy voxel greater than 0.5, because we did not know *a priori* the extent to which contamination of the spectrum with metabolites in brain would affect the ability of ^{1}H-MR spectroscopy to characterize tumors.

Histopathology reports were reviewed independently at Fox Chase Cancer Center to ascertain the diagnosis and to confirm typing of glial tumors according to the current World Health Organization (WHO) classification:[27] astrocytic tumors, oligodendrogliomas, and ependymomas. Astrocytic tumors were subclassified according to increasing grade of malignancy as astrocytoma (AS), anaplastic astrocytoma (AA), and glioblastoma multiforme (GBM). In approximately two-thirds of the cases, pathologists used this classification explicitly. In the remainder, the previous WHO or other classifications that used numerical grading (I–IV) were used. However, typical GBM and typical low-grade AS were readily identified. Thus, less than 10% of astrocytic tumors originally had been designated "Grade III" or "Grade III–IV" and required reassignment to current WHO typing. If there was any necrosis or vascular proliferation within tumor-containing regions in the microscopic description, the case was designated GBM. Four cases in which current WHO typing was not used and whose microscopic description was inadequate to permit independent assignment were excluded from further analysis.

Recurrent tumor cases were evaluated to ascertain independently the strength of the evidence for recurrence and, in cases previously treated, the ability to separate the region of tumor from regions of radiation or surgical damage. Information used to make these judgments included the MR imaging studies (with and without contrast enhancement), computerized tomography scans, and recently repeated biopsies. If objective evidence for recurrent tumor could not be ascertained, the case was excluded from further analysis.

Proton ^{1}H-Magnetic Resonance Spectroscopy

Scout MR images using fast low-angle shot (FLASH)[18] were obtained in two or three planes through the brain to define the region of placement of 8-cc MR spectroscopy voxels. Voxels were placed to maximize their content of viable tumor. Necrotic or cystic regions of tumors were avoided when possible but were included in the voxel if necessary to limit brain contamination. Wherever feasible, ^{1}H-NMR spectra were obtained both from the tumor and the mirror-image region in the contralateral brain. Global and localized shimming on the water proton was performed to obtain less than 25 Hz and 10 Hz full width at half-maximum, respectively, from brain. Spectra were localized using the spin-echo method[7] along with chemical shift selective water suppression.[17] A single-voxel method, rather than multivoxel chemical shift imaging, was selected because of the feasibility of implementation in clinical imagers at multiple institutions. The spin-echo method was selected based partly because of its signal-to-noise advantage over the stimulated echo method.[37] The advantages and limitations of this method have been discussed.[48,55] Different regions of the spectrum have signals emitting from slightly different voxels: those of cholines at 3.2 ppm are from a voxel whose dimensions are each shifted approximately 10% relative to those of lipids at

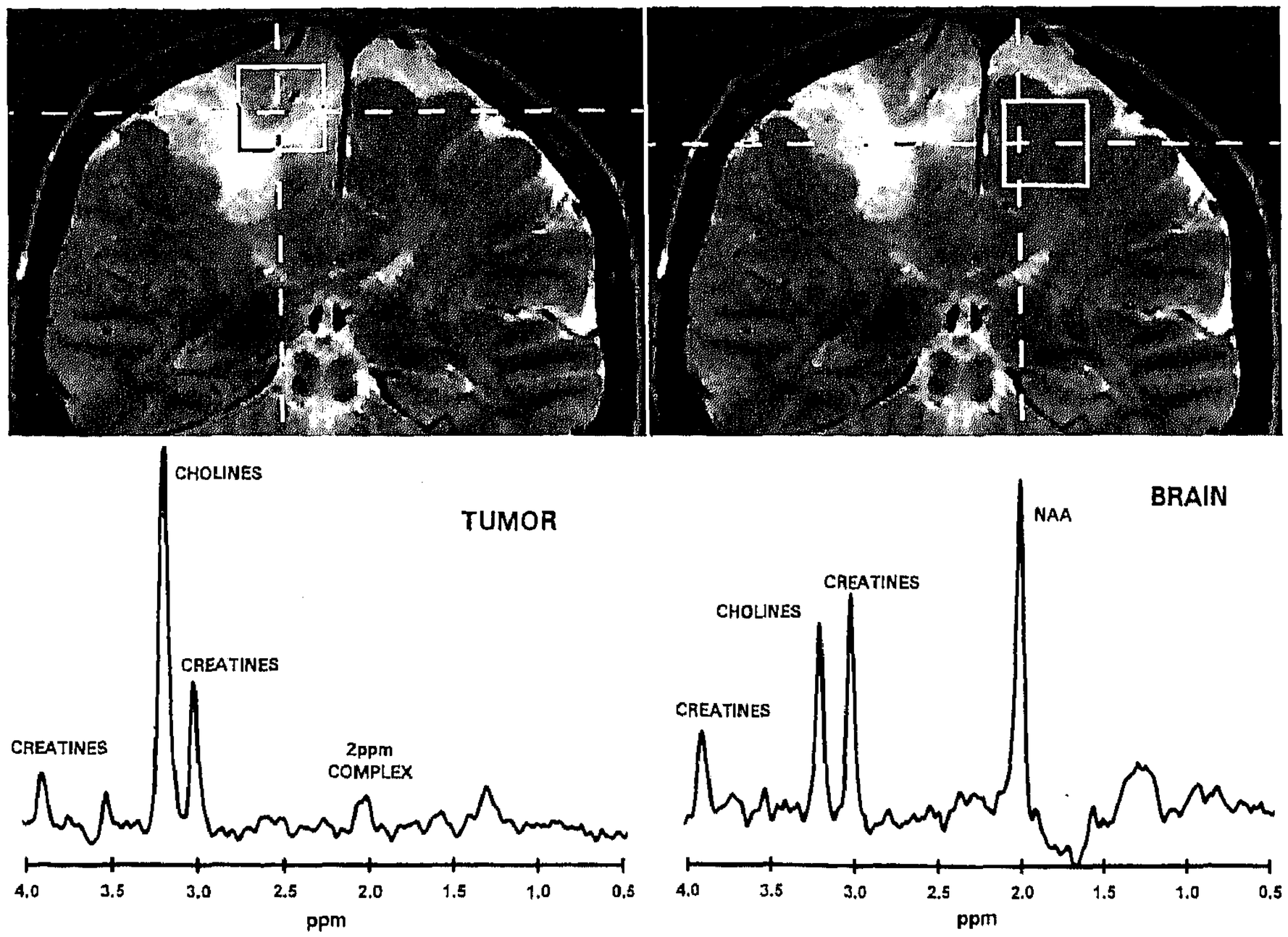

FIG. 2. Magnetic resonance (MR) spectroscopy voxel locations and ^{1}H-MR spectra in a patient with an astrocytic tumor in the right parietal lobe. *Upper Left:* A T_2-weighted MR image showing the position of the 2 × 2 × 2 cm voxel centered in the tumor. *Upper Right:* A T_2-weighted MR image showing the position of the 2 × 2 × 2 cm voxel in the contralateral brain. *Lower Left* and *Right:* Charts displaying ^{1}H-MR spectra from the tumor *(lower left)* and the contralateral brain *(lower right)*.

0.9 ppm. Chemical shift dispersion reduces the effective voxel size for lactate to 5.6 ml when the nominal voxel size for singlet resonances is 8 ml. This, along with imperfections in rectangular slice profiles and effects of multiple quantum coherences by variations in pulse angles, results in approximately a 50% reduction in sensitivity of the spin-echo method for lactate.

Two-hundred fifty-six acquisitions were obtained with an echo time of 135 msec and a repetition time of 1600 msec to give a total MR spectroscopy acquisition time of 6.5 minutes. The echo time of 135 msec was used so that, relative to the remainder of the spectrum, lactate methyl proton signals would be 180° out of phase whereas intratumoral lipid methylene proton signals (which overlap lactate at 1.3 ppm) would be in phase. Phase distortions in the water-suppressed ^{1}H-NMR spectrum caused by eddy currents were removed by taking a nonsuppressed water reference signal acquired with the same MR spectroscopy sequence and calculating a phase transformation factor, permitting one to set the phase angle to zero for each time point.[28,42] The ^{1}H-MR spectroscopy procedure is illustrated in Fig. 2, in which MR spectroscopy voxel positions are overlaid on scout MR images and spectra from tumor and brain are shown.

Analysis of Data From MR Spectroscopy

Digital MR spectroscopy data were submitted for blinded analysis to Siemens, AG (Erlangen, Germany). Peak areas were determined by manual integration using Siemens Numaris software. Peaks were assigned according to their positions relative to water at 4.7 ppm and metabolite identification *in vitro*.[31,36,49] Brain spectra (Fig. 2) contain four peaks: one primarily from the *N*-trimethyl protons of choline-containing metabolites at 3.2 ppm, one from the *N*-methyl protons of creatines at 3.0 ppm, a smaller one from the methylene protons of creatine at 3.9 ppm, and one primarily from the methyl protons of NAA at 2.0 ppm. *N*-acetylaspartate is within neurons and therefore is decreased whenever the brain is damaged or replaced. In tumors the peak around 2.0 ppm may then contain larger fractions of metabolites present in concentrations normally much lower than that of NAA, including *N*-acetyl-aspartylglutamate, glutamine, glutamate, and γ-aminobutyric acid. Therefore, in tumors we refer to the "NAA region" rather than to "NAA."

The MR spectroscopy data are presented in two ways. First, the peak area intensity of the signal of each metabolite in the tumor was expressed as a ratio to the intensity of creatines in contralateral brain. Assuming brain creatines to be an appropriate reference and ignoring any possible saturation effects, this permits estimation of the extent to which metabolite concentrations are altered in tumors. Second, peak area intensities of intratumoral metabolites were expressed as ratios to one another and compared to the same ratios in contralateral brain and in other tumor types. Mean ratios were compared between groups by nonparametric tests to take into account nonnormal distributions within some of the groups. The Mann–Whitney U-test was used for nonpaired group comparisons and the Wilcoxon signed-rank test for paired

TABLE 1

*Selection and exclusion within 113 cases of patients with glial tumors on MR spectroscopy**

Case Selection	No. of Cases
cases with MR spectroscopy data submitted	113
cases excluded from analysis	27
MR spectrum of poor quality	12
<0.5 tumor/tumor + brain in voxel	11
insufficient histopathological description	4
cases evaluated	86
cases with spectra from contralateral brain	41

* MR = magnetic resonance.

group comparisons. Analysis of variance was used to compare metabolite ratios across histopathological grades and Fisher's exact test to compare incidences of lipids and lactate in tumor subgroups.

Results

Fifteen institutions studied 113 patients with glial tumors over approximately 1 year. Application of the evaluation algorithm (Fig. 1) resulted in the exclusion of 27 cases (Table 1). The 86 cases selected for evaluation included 75 astrocytic tumors, six oligodendrogliomas, and five ependymomas. Of the 19 ASs, five were pilocytic, one was a subependymal giant cell, and one a mixed oligoastrocytoma. Of the 22 AAs, one was a mixed oligoastrocytoma. Diagnoses, demographic data, relevant clinical data, and results of independent analysis of MR spectroscopy voxel compositions are summarized in Table 2. Thirteen glial tumors were found in children (< 18 years old); nine of these tumors were astrocytic and four were ependymomas. Of 55 newly diagnosed cases, only seven patients had had biopsy before MR spectroscopy was performed. Of 31 recurrent tumors, 25 had previously been treated with radiation therapy.

The effect of voxel contamination on the ratios of the levels of cholines, creatines, and the NAA region in astrocytic tumors to those of the corresponding metabolites in brain is shown in Fig. 3. As expected, the mean intensity of the NAA region in tumors relative to that in the contralateral brain decreased progressively with decreasing brain contamination. The mean intensity of creatines in tumors relative to that in the contralateral brain was slightly reduced, but did not decrease progressively with decreasing brain contamination. The mean intensity of cholines in tumors relative to that in the contralateral brain was much higher in cases with tumor fractions of 0.7 to 0.8 or 0.9 to 1.0 than in cases with tumor fractions of 0.5 to 0.6. Therefore, in subsequent analyses, we included only cases with voxels containing tumor fractions of at least 0.7.

The results in Fig. 3 indicate that the concentration of choline is increased and that of creatine is slightly decreased in glial tumors compared to brain. The effect of the histopathological grade of the tumor on metabolite concentrations, expressed as the ratio of their peak area intensities to those of creatines in the contralateral brain, is shown in Fig. 4 and statistical comparisons are given in the figure legend. The mean intensity of cholines was significantly higher in AS and AA compared to brain but not significantly higher in GBM compared to brain. The mean intensity of creatines was the same in AS as in brain but decreased progressively with the increasing histopathological grade of the astrocytic tumor. The mean intensity of the NAA region was decreased in all tumor types.

The results displayed in Fig. 4 indicate that the overlap of metabolite signal intensities or of concentrations among grades of astrocytic tumors is too great to provide

TABLE 2

*Characteristics of 86 cases evaluated**

Characteristic	Glial (86 cases)	AS (19 cases)	AA (22 cases)	GBM (34 cases)	OD (6 cases)	EP (5 cases)
age of patients (yrs)						
mean	41	30	43	51	35	14
range	3–75	5–73	3–72	18–75	30–39	4–30
gender						
male	51	11	13	21	4	2
female	35	8	9	13	2	3
tumor status						
new	55	14	12	21	3	5
recurrent	31	5	10	13	3	0
prior radiation	25	4	9	11	1	0
fraction of tumor in voxel						
0.5–0.6	14	5	1	7	1	0
0.7–0.8	28	3	8	14	1	2
0.9–1.0	44	11	13	13	4	3

* Abbreviations: AA = anaplastic astrocytoma; AS = astrocytoma; EP = ependymoma; GBM = glioblastoma multiforme; OD = oligodendroglioma.

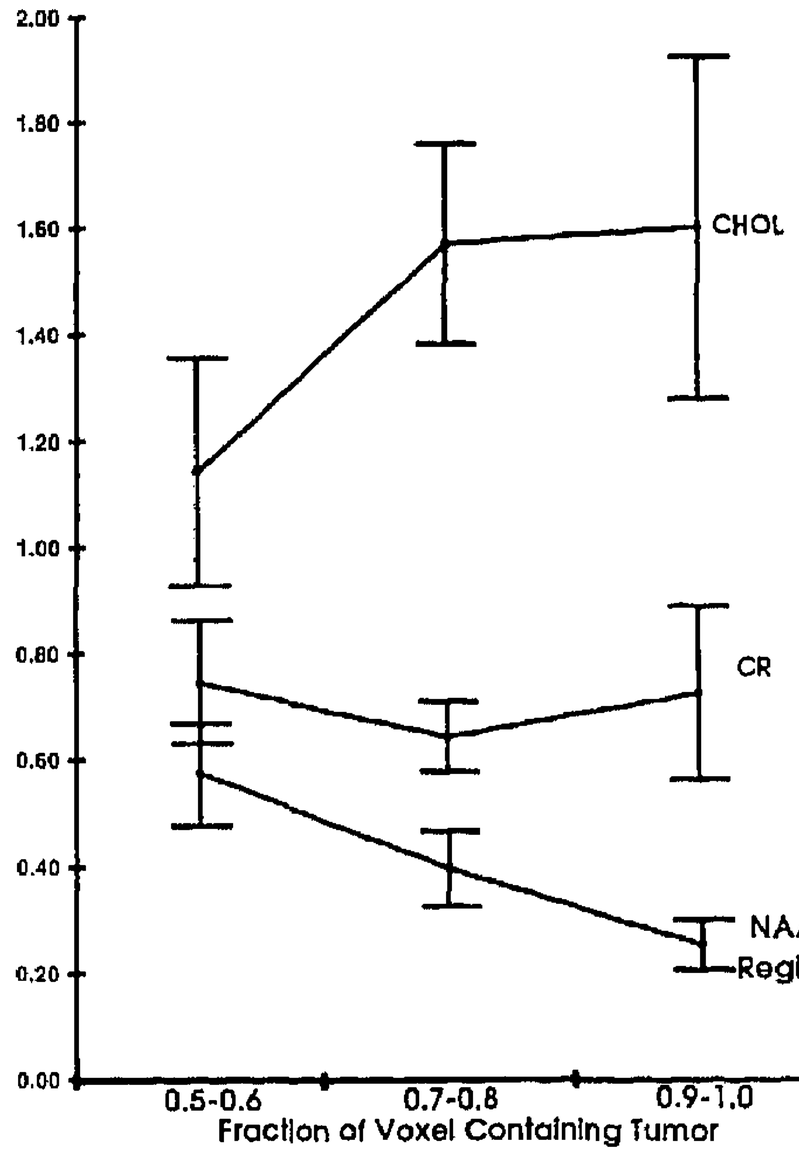

FIG. 3. Graph depicting the effect of voxel contamination by brain on ratios of metabolite signal intensities in tumors to those in contralateral brain. The fractions of tumor within the magnetic resonance spectroscopy voxels are indicated. Values are expressed as means ± standard error. CHOL = choline; CR = creatine; NAA = *N*-acetylaspartate.

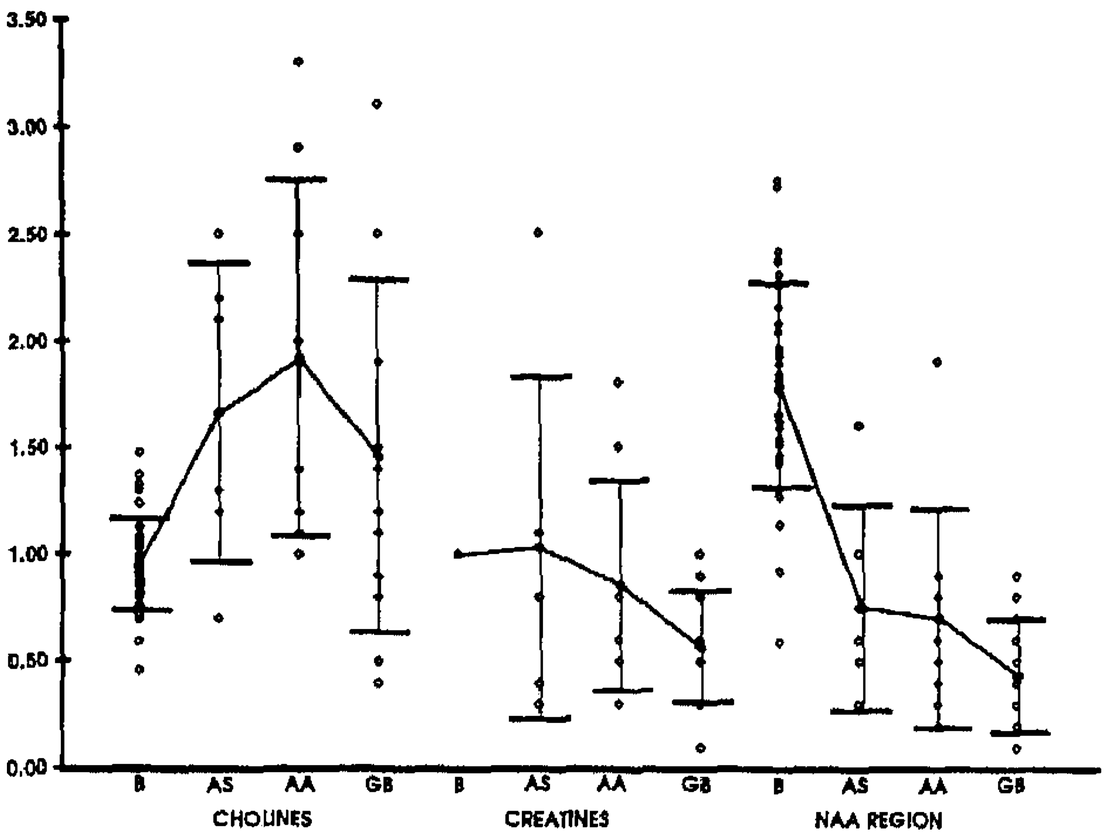

FIG. 4. Graph displaying the means, standard deviations, and scatterplot of cholines, creatines, and *N*-acetylaspartate (NAA) region in astrocytic tumors expressed as ratios to the creatine peak intensities in contralateral brain. AA = anaplastic astrocytomas; AS = astrocytomas; B = brain; GB = glioblastomas multiforme. Significance of differences (p) compared to brain: for cholines, AS 0.0014, AA 0.0002, and GB 0.1905; for creatines, AS 0.9999, AA < 0.0001, and GB 0.0001; for NAA region, AS, AA, and GB < 0.0001.

any diagnostic accuracy. Therefore, we examined the ratios between any two metabolites within the same tumor and the results are summarized in Table 3. All major types of glial tumors had significantly higher mean choline/creatine and choline/NAA ratios, and a lower mean NAA/creatine ratio, compared to brain. Among tumor subtypes, AA had a significantly higher mean choline/creatine ratio than AS. However, the variations and overlaps among the tumor types remained large.

The spectrum of a tumor containing lactate is shown in Fig. 5 *left*. It appears as a doublet 180° out of phase centered at 1.3 ppm. The spectrum of a tumor containing

TABLE 3

*Comparison of metabolic ratios in glial tumors to those in contralateral brain spectra in unpaired observations**

Sample	Choline/Creatine Ratio	NAA Region/ Creatine Ratio	Choline/NAA Region Ratio
brain (41 cases)	0.97 ± 0.22	1.78 ± 0.48	0.59 ± 0.23
astrocytoma (14 cases)	2.13 ± 0.82†	0.78 ± 0.44†	2.52 ± 1.29†
anaplastic astrocytoma (21 cases)	2.82 ± 1.45†‡	0.99 ± 0.58†	3.29 ± 2.17†
glioblastoma multiforme (27 cases)	2.77 ± 1.93†	0.89 ± 0.43†	3.99 ± 3.75†
oligodendroglioma (4 cases)	5.00 ± 3.96§	1.03 ± 0.63‖	6.53 ± 6.13**
ependymoma (5 cases)	2.80 ± 0.49††	0.98 ± 0.42‡‡	3.96 ± 3.27**

* Eight tumors exhibited no quantifiable creatines, hence infinitely high ratios of cholines or of NAA region to creatines are not included in this table. Values are expressed as means ± standard deviations with p values for tumors compared to brain based on the Mann–Whitney U-test. NAA = *N*-acetylaspartate.

† $p < 0.0001$; ‡ $p = 0.0264$ for anaplastic astrocytoma compared to astrocytoma; § $p = 0.0009$; ‖ $p = 0.0358$; ** $p = 0.0100$; †† $p = 0.0003$; ‡‡ $p = 0.0028$.

TABLE 4

Incidence of lipids and lactate in 86 glial tumors

Tumor Type	Total No. of Cases	Lipids No. (%)	Lactate No. (%)
astrocytic tumors	75	26 (35)	9 (12)
astrocytoma	19	3 (16)	4 (21)
anaplastic astrocytoma	22	8 (36)	1 (5)
glioblastoma multiforme	34	15 (44)	4 (12)
prior radiation	24	11 (46)	3 (13)
no radiation	51	15 (29)	6 (12)
oligodendroglioma	6	0	0
ependymoma	5	0	1 (20)

mobile lipids is shown in Fig. 5 *right*. The fatty acyl-CH_2 peak is at 1.3 ppm and the acyl-CH_3 peak is at 0.9 ppm. Lipid signals from skull or scalp were distinguished from intratumoral lipids by: 1) a voxel position near the skull; 2) similar contamination in the contralateral brain spectrum; and 3) anomalous phase errors and/or chemical shifts. By these criteria, the small lipid signal at 1.3 ppm in the tumor shown in Fig. 2 is assumed to be contamination from skull or scalp.

The incidences of lipids and lactate in the major tumor types are shown in Table 4. Lipids occurred in 41% of AAs and GBMs but in only 16% of ASs. These incidences may be lower than actual ones because we did not include two cases in which it was not possible to separate lipid from lactate and 14 cases in which signals in the 0.5 to 1.7 ppm region, judged to have resulted only from contamination, could have masked intratumoral lipids or lactate. The relation between lipid signal intensity and histopathological grade of astrocytic tumors is shown in Fig. 6. The mean level of 1.3 ppm/choline in GBMs with lipids (3.2 ± 3.1 standard deviation (SD)) was higher than those in AAs with lipids (1.8 ± 1.7) and in ASs with lipids (0.5 ± 0.4; $p = 0.0503$). Lactate was detected in only nine of the 75 astrocytic tumors and in one of the five ependymomas, and occurred in low- as well as high-grade tumors (four ASs, one AA, and four GBMs).

New and recurrent astrocytic tumors had identical mean choline/creatine ($p = 0.90$) and NAA/creatine ratios ($p = 0.92$). The 25 tumors treated with prior radiation had a mean choline/creatine ratio of 2.5, not unlike that of nonradiated tumors (2.6; $p = 0.77$). The incidence of lactate was the same in radiated and nonradiated astrocytic tumors (Table 4). Lipids occurred more frequently in radiated tumors (0.46) than in nonradiated ones (0.29), but this difference was not significant ($p = 0.198$) and may reflect the higher grade of recurrent tumors. Therefore, metabolic changes associated with radiation did not confound our results, possibly because of the effort made to ensure the presence of viable tumor in the MR spectroscopy voxel in all cases.

Discussion

This study shows that a multiinstitutional cooperative trial of ^{1}H-MR spectroscopy is feasible. It enabled accrual of a large number of cases in a short period of time, approximately 1 year for most of the institutions. Because this was one of the first attempts to perform such a trial,

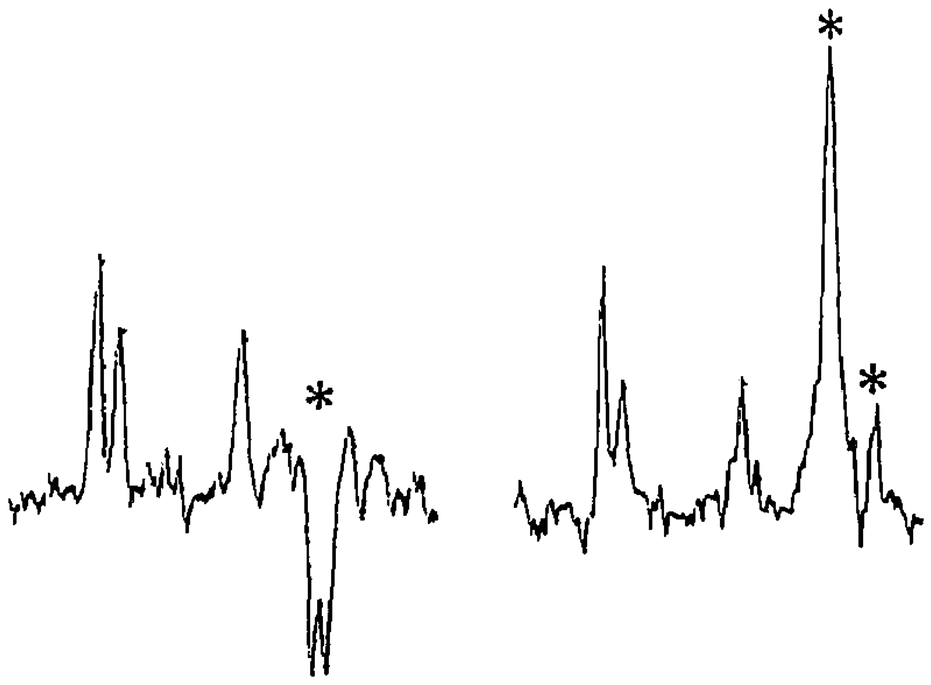

FIG. 5. Examples of spectra with lipids or lactate. *Left:* Lactate-CH_3 appears as an inverted doublet at 1.3 ppm *(asterisk). Right:* Lipids with the dominant fatty acyl-CH_2 peak at 1.3 ppm and the -CH_3 at 0.9 ppm *(asterisks).*

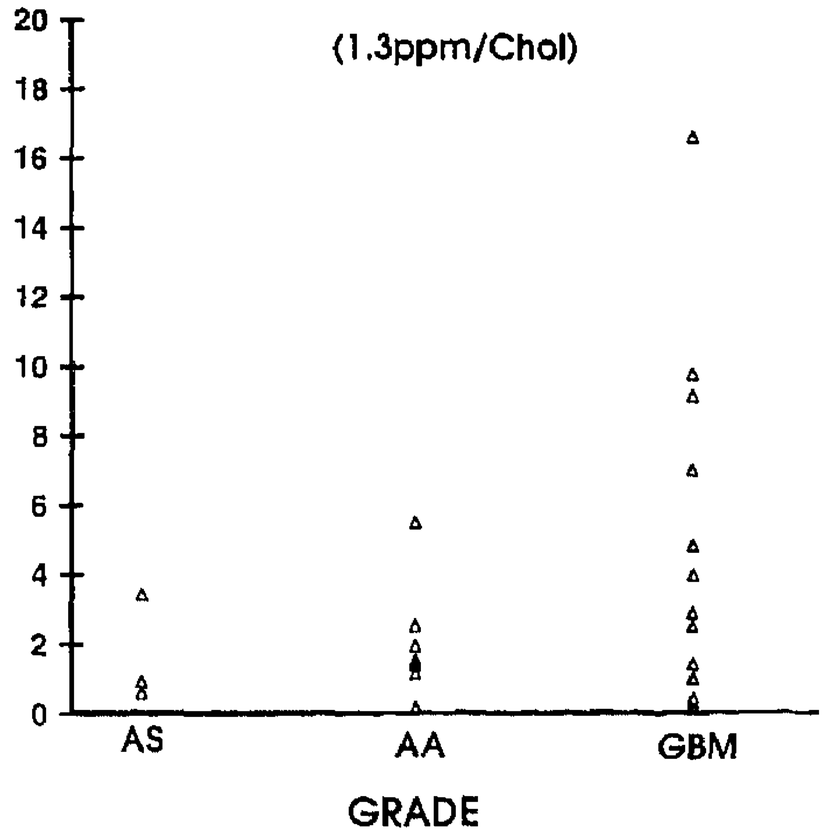

FIG. 6. Graph showing lipids in astrocytic tumors, expressed as the ratio of intensity of the 1.3 ppm methylene peak to that of cholines (Chol). AA = anaplastic astrocytomas; AS = astrocytomas; GBM = glioblastomas multiforme.

ours has been a learning experience and the clinical quality assurance procedures (Fig. 1) were applied retrospectively. This and our insistence on independent, central review of imaging, histopathological reporting, and clinical data may account for the relatively large number of cases excluded from analysis. However, if quality-assurance criteria established during this study were applied prospectively rather than retrospectively, and if voxel sizes smaller than 8 cc were permitted, it should be possible to increase the number of cases that could be evaluated.

The major observations of this study are: 1) elevated mean signal intensities of cholines, and decreased intensities of creatines and the NAA region in glial tumors compared to contralateral brain; 2) intratumoral lipids in 41% of higher grade (AA and GBM) astrocytic tumors, the mean amount higher in GB than AA; and 3) infrequent occurrence of lactate with no relation to histopathological grade. The elevated choline/creatine ratio in primary glial brain tumors in general, observed here and in some studies in the literature (discussed below), is caused by increased signal intensities of cholines and decreased signal intensities of creatines compared to brain. Contamination of the MR spectroscopy voxel by brain has a marked effect on metabolite intensities and ratios, but selection of cases in which the MR spectroscopy voxel contained a relatively low amount (< 30%) of contamination did not overcome the large variations within, or overlaps between, the three histopathological grades of astrocytic tumors.

The mean metabolite ratios in contralateral brain (0.97 for choline/creatine and 1.78 for NAA/creatine) are similar to those in the normal volunteer study[53] to which each of the institutions in our trial contributed spectra from a designated position in the parietooccipital lobe (0.81 for choline/creatine and 2.16 for NAA/creatine) and the caudate nucleus (0.95 for choline/creatine and 1.87 for NAA/creatine). The coefficients of variations are also similar to those observed in the volunteer study: 23% for choline/creatine compared to 19% in parietooccipital lobes and 20% in caudate nuclei; and 27% for NAA/creatine compared to 19% in parietooccipital lobes and 29% in caudate nuclei. This result indicates that overall technical quality control established in the volunteer study was maintained by the institutions in this patient study. Therefore, the much greater variations of choline and creatine metabolite ratios observed in glial tumors may be the result of greater metabolic differences between them. Each type and grade of tumor appears to represent a metabolically heterogeneous group.

The microscopic or biological basis for metabolic heterogeneity within solid or apparently viable tumor is not clear. Some astrocytic tumors are not distinct solid masses but rather infiltrate brain tissue[27] that produces the NAA signals observed even when little evident brain is within the voxel (Fig. 3). Many benign ASs contain foci of anaplastic cells,[50,54] and GBMs containing foci of ASs have a better prognosis than GBMs not containing ASs.[62] Heterogeneity of metabolic characteristics and of cellular necrosis in astrocytic tumors[30,31] and heterogeneity of blood volume *in vivo* in high-grade astrocytomas[5] occur on a scale less than 0.1 ml, much smaller than the smallest ^{1}H-MR spectroscopy voxel currently feasible (approximately 1 cc). Heterogeneity found over this scale could explain why studies using multiple small ^{1}H-MR spectroscopy voxels localized by two-dimensional chemical shift imaging[14,15,20,22] have not demonstrated less scatter within, or less overlap between, grades of glial tumors than our studies and others using single large voxels. Combinations of chemical shift imaging using molar quantitation[3,24,29,35] and short-echo[3,12,34,35,46,60] techniques to obtain metabolic information heretofore observed only *in vitro*[16,26,45,59,61] or *ex vivo*[30,31,51] might improve the specificity of ^{1}H-MR spectroscopy. However, Preul, *et al.*,[47] have been able to overcome the scatter within each metabolic peak and distinguish brain tumor subtypes with very high specificity by applying a linear discriminant to analyze the patterns of all of the peak intensities in spectra obtained at a long (270 msec) echo time. To achieve this result, they studied only untreated cases and selected from two-dimensional chemical shift imaging datasets voxels that appeared to be most representative of viable tumor.

Some of the previous studies that focused on metabolite ratios *in vivo* in different histopathological grades of astro-

cytic tumors reported a higher choline/creatine ratio in high- compared to low-grade tumors,[4,21,43,57,58,61] but three found this ratio unchanged[11] or reduced[14,32] in high grades such as GBM compared to intermediate grades such as AA. The mean choline/creatine ratio we observed in astrocytic tumors with minimal brain contamination is higher than in many previous reports and is similar to the result of Ott and colleagues[43] who used a similar ^{1}H-MR spectroscopy technique to examine 48 astrocytic tumors and minimized contamination by varying voxel size to fit the region of solid, apparently viable tumor.

Comparisons between tumors and contralateral brain indicated that the higher mean ratios of levels of cholines to creatines and the NAA region in AAs and GBMs compared to lower grade ASs (Table 3) is caused partly by higher concentrations of cholines and partly by lower concentrations of creatines and of the NAA region (Fig. 4). These results in general are in accord with those obtained in surgical specimens assayed biochemically[33] or with ^{1}H-NMR spectroscopy.[16,45,61] The lower creatine concentration in GBMs compared to lower grade astrocytic tumors, and the lack of a higher concentration of cholines in GBMs compared to lower grade tumors (Fig. 4), were also observed *in vivo* in other studies in which both tumor and brain spectra were obtained from the same subjects.[11,14,43]

The infrequent occurrence of lactate (12% of all glial tumors) and the lack of a correlation with histopathological grade agrees with Ott and colleagues,[43] who reported a definite lactate resonance in only 19% of 75 spectra from 48 astrocytic tumors. It is possible that both we and Ott and colleagues underestimated the incidence of lactate because our techniques have a lower sensitivity to lactate than to singlet resonances and because in a few cases high lipid signals could mask small amounts of lactate. Kugel, *et al.*,[32] reported lactate in nine (41%) of 22 glial tumors, but also found that it occurred equally in low- and high-grade tumors. Fulham, *et al.*,[14] reported lactate in 18 (41%) of 44 glial tumors, occurring with significantly higher incidence in higher grades. However, 13 of the 18 tumors with lactate had been treated, and the lactate was generally observed at the site of surgery and in subacute radiation necrosis; thus in many cases viable tumor may not have been the source of the lactate. Our results do contradict the conclusions of several previous studies,[2,4,8,15,20–22] some of which may have overestimated the incidence of lactate because of their inability to distinguish lactate from lipids.

Methylene and methyl signals were described in glial tumors studied with ^{1}H-MR spectroscopy using short echo times,[12,46,60] and Tzika and associates[60] assigned lipids to the spectra of virtually all childhood brain tumors of various types and grades. With short echo times, however, these signals may also arise from proteins.[6] One criterion that may be applied to help distinguish protein from lipid signals is that the latter, which are from fatty acyl chains, should have a relatively high ratio of the intensity of the methylene peak at 1.3 ppm compared to that of the methyl peak at 0.9 ppm.[31,51] In our cases with lipids (for example, Fig. 5 *right*), this ratio averaged 5.6 (± 2.8 SD), and because the T_2 relaxation times are similar,[31] a similar ratio should occur at short echo time. By this criterion, Tzika and associates[60] have greatly overestimated the incidence of lipids in brain tumors and other disorders.

We have demonstrated the presence of mobile lipids in a significant fraction of astrocytic tumors and defined their relation to histopathological grade. These observations provide a correlation *in vivo* of the recent documentation of lipids in ^{1}H-NMR spectroscopy studies of intact surgical specimens of brain tumors.[30,31,51] Kuesel and coworkers[30,31] showed that the amount of mobile lipids in higher grade astrocytic tumors correlated with the amount of microscopic cellular necrosis within the specimen. The lipid signals observed by ^{1}H-MR spectroscopy arise predominantly from fatty acyl moieties, which are relatively mobile and probably no longer confined to membrane phospholipids. Their association with cellular necrosis in GBMs is probably due to membrane breakdown. Because we observed lipids in eight of 22 AAs, which by definition[27] contain little or no necrosis, we suggest that membrane breakdown may precede histologically evident necrosis. Indeed, Kuesel, *et al.*,[30] suggested that the appearance of mobile lipids in regions of viable tumor indicates metabolic effects of poor perfusion, and neutral lipid droplets were detected in the cytoplasm of hypoxic tumor cells.[13]

Large amounts of lipids appear to be specific for AA or GBM, but their absence does not rule out AA or GBM. However, it is important to note that histopathological grading is imperfect in its correlation with prognosis. In adults in particular, the clinical course of lower grade tumors, more than half of which recur as, or evolve into, an aggressive phenotype, is difficult to predict.[38] Therefore, even if ^{1}H-MR spectroscopy metabolic characteristics have limited diagnostic accuracy, they may have prognostic significance, as has been found in the case of glucose hypermetabolism in PET.[1,23,25,44,56] Current issues in the management of patients with AS are whether or not there is an advantage to gross-total resection and whether or not postoperative radiotherapy influences the rate of differentiation or relapse.[38] A metabolic characteristic that independently correlates with malignant behavior could help the clinician to balance the risks and benefits of aggressive therapy more accurately. Because microscopic necrosis in GBM does correlate with prognosis,[9,10,41] it is possible that the presence of lipids will also. Moreover, because the appearance of mobile lipids appears to precede evident necrosis,[30] it is possible that their presence in AAs will provide a marker for tumors likely to evolve into more aggressive behavior. Therefore, the population that has been accrued in this trial will be followed over the next few years to obtain relapse-free and overall survival statistics. This may enable us to determine if the presence of lipids or other metabolic characteristics (for example, choline concentrations that are above median vs. those below median) predicts prognosis independent of histopathological grade.

Acknowledgments

We thank Siemens Medical Systems for its support and encouragement of the group effort, and Drs. Annette C. Kuesel and Michael Garwood for helpful discussions.

Appendix

Institutions and Participants in the Study

Participating Medical Facilities

Austria

E. Moser, S. Aull, G. Gomiscek, K. Heimberger, C. Matula,

N. Pfafflmeyer, R. Radlbauer, K. Roessler,
University of Vienna, Vienna
Germany
T. J. Vogl, O. Soellner, Free University, Berlin
B. Terwey, Saint Juergen Street Central Hospital, Bremen
Greece
E. D. Gotsis, Encephalos Institute, Halandri
Italy
A. Falini, G. Scotti, and F. Triulzi, San Raffaele Scientific Institute, Milan
Japan
K. Kamada, Hokkaido University, Sapporo
The Netherlands
A. Heerschap, A. de Koster, R. van der Maazen, H. Thijssen, University Hospital, Nijmegen
United States
M. M. Mengeot, D. Elias, T. Helenowski, J. Leestma, Chicago Institute of Neurosurgery and Neuroresearch, Chicago, Illinois
R. A. Zimmerman, J. Haselgrove, L. N. Sutton, Z. Wang, Children's Hospital of the University of Pennsylvania, Philadelphia, Pennsylvania
B. C. P. Lee, M. Crowley, Mallinkrodt Institute, St. Louis, Missouri
W. G. Negendank, T. R. Brown, K. A. Padavic-Shaller, F. Arias-Mendoza, Fox Chase Cancer Center, Philadelphia, Pennsylvania
A. E. Stillman, J. Grad, W. Hall, University of Minnesota, Minneapolis, Minnesota
J. A. Sanders, University of New Mexico, Albuquerque, New Mexico
T. A. Spraggins, University of Virginia, Charlottesville, Virginia
J. L. Evelhoch, G. Barger, Wayne State University, Detroit, Michigan
Manufacturer
R. Sauter, K. Wicklow, Siemens, AG, Erlangen, Germany

References

1. Alavi JB, Alavi A, Chawluk J, et al: Positron emission tomography in patients with glioma. A predictor of prognosis. **Cancer 62:**1074–1078, 1988
2. Alger JR, Frank JA, Bizzi A, et al: Metabolism of human gliomas: assessment with H-1 MR spectroscopy and F-18 fluorodeoxyglucose PET. **Radiology 177:**633–641, 1990
3. Alger JR, Symko SC, Bizzi A, et al: Absolute quantitation of short TE brain ^{1}H-MR spectra and spectroscopic imaging data. **J Comput Assist Tomogr 17:**191–199, 1993
4. Arnold DL, Shoubridge EA, Villemure JG, et al: Proton and phosphorus magnetic resonance spectroscopy of human astrocytomas *in vivo*. Preliminary observations on tumor grading. **NMR Biomed 3:**184–189, 1990
5. Aronen HJ, Gazit IE, Louis DN, et al: Cerebral blood volume maps of gliomas: comparison with tumor grade and histologic findings. **Radiology 191:**41–51, 1994
6. Behar KL, Ogino T: Characterization of macromolecule resonances in the ^{1}H NMR spectrum of rat brain. **Magn Reson Med 30:**38–40, 1993
7. Bottomley PA: Spatial localization in NMR spectroscopy *in vivo*. **Ann NY Acad Sci 508:**333–348, 1987
8. Bruhn H, Frahm J, Gyngell ML, et al: Noninvasive differentiation of tumors with use of localized H-1 MR spectroscopy *in vivo*: initial experience in patients with cerebral tumors. **Radiology 172:**541–548, 1989
9. Burger PC, Vogel FS, Green SB, et al: Glioblastoma multiforme and anaplastic astrocytoma. Pathologic criteria and prognostic implications. **Cancer 56:**1106–1111, 1985
10. Daumas-Duport C, Scheithauer B, O'Fallon J, et al: Grading of astrocytomas. A simple and reproducible method. **Cancer 62:** 2152–2165, 1988
11. Demaerel P, Johannik K, Van Hecke P, et al: Localized ^{1}H NMR spectroscopy in fifty cases of newly diagnosed intracranial tumors. **J Comput Assist Tomogr 15:**67–76, 1991
12. Frahm J, Bruhn H, Hänicke W, et al: Localized proton NMR spectroscopy of brain tumors using short-echo time STEAM sequences. **J Comput Assist Tomogr 15:**915–922, 1991
13. Freitas I, Pontiggia P, Barni S, et al: Histochemical probes for the detection of hypoxic tumour cells. **Anticancer Res 10:** 613–622, 1990
14. Fulham MJ, Bizzi A, Dietz MJ, et al: Mapping of brain tumor metabolites with proton MR spectroscopic imaging: clinical relevance. **Radiology 185:**675–686, 1992
15. Furuya S, Naruse S, Ide M, et al: [The clinical application of multi-voxel ^{1}H-CSI (chemical shift imaging) in brain tumors.] **Nippon Igaku Hoshasen Gakkai Zasshi 51:**836–838, 1991 (Jpn)
16. Gill SS, Thomas DGT, Van Bruggen N, et al: Proton MR spectroscopy of intracranial tumours: *in vivo* and *in vitro* studies. **J Comput Assist Tomogr 14:**497–504, 1990
17. Haase A, Frahm J, Hänicke W, et al: ^{1}H NMR chemical shift selective (CHESS) imaging. **Phys Med Biol 30:**341–344, 1985
18. Haase A, Frahm J, Matthaei D, et al: FLASH imaging. Rapid NMR imaging using low flip-angle pulses. **J Magn Reson 67:** 258–266, 1986
19. Hasso AN: Current status of enhanced magnetic resonance imaging in neuroradiology. **Invest Radiol 28 (Suppl 1):**S3–S20, 1993
20. Heesters MAAM, Kamman RL, Mooyaart EL, et al: Localized proton spectroscopy of inoperable brain gliomas. Response to radiation therapy. **J Neurooncol 17:**27–35, 1993
21. Henriksen O, Wieslander S, Gjerris F, et al: *In vivo* ^{1}H-spectroscopy of human intracranial tumors at 1.5 Tesla. Preliminary experience at a clinical installation. **Acta Radiol 32:**95–99, 1991
22. Herholz K, Heindel W, Luyten PR, et al: *In vivo* imaging of glucose consumption and lactate concentration in human gliomas. **Ann Neurol 31:**319–327, 1992
23. Hölzer T, Herholz K, Jeske J, et al: FDG-PET as a prognostic indicator in radiochemotherapy of glioblastoma. **J Comput Assist Tomogr 17:**681–687, 1993
24. Husted CA, Duijn JH, Matson GB, et al: Molar quantitation of *in vivo* proton metabolites in human brain with 3D magnetic resonance spectroscopic imaging. **Magn Reson Imaging 12:** 661–667, 1994
25. Kim CK, Alavi JB, Alavi A, et al: New grading system of cerebral gliomas using positron emission tomography with F-18 fluorodeoxyglucose. **J Neurooncol 10:**85–91, 1991
26. Kinoshita Y, Kajiwara H, Yokota A, et al: Proton magnetic resonance spectroscopy of brain tumors: an *in vitro* study. **Neurosurgery 35:**606–613, 1994
27. Kleihues P, Burger PC, Scheithauer BW: **Histological Typing of Tumours of the Central Nervous System, ed 2.** Berlin: Springer-Verlag, 1993
28. Klose U: *In vivo* proton spectroscopy in presence of eddy currents. **Magn Reson Med 14:**26–30, 1990
29. Kreis R, Ernst T, Ross BD: Absolute quantitation of water and metabolites in the human brain. II. Metabolite concentrations. **J Magn Reson (B) 102:**9–19, 1993
30. Kuesel AC, Donnelly SM, Halliday W, et al: Mobile lipids and metabolic heterogeneity of brain tumours as detectable by *ex vivo* ^{1}H MR spectroscopy. **NMR Biomed 7:**172–180, 1994
31. Kuesel AC, Sutherland GR, Halliday W, et al: ^{1}H MR spectroscopy of high grade astrocytomas: mobile lipid accumulation in necrotic tissue. **NMR Biomed 7:**149–155, 1994
32. Kugel H, Heindel W, Ernestus RI, et al: Human brain tumors: spectral patterns detected with localized H-1 MR spectroscopy. **Radiology 183:**701–709, 1992
33. Lowry OH, Berger SJ, Chi MY, et al: Diversity of metabolic patterns in human brain tumors—I. High energy phosphate compounds and basic composition. **J Neurochem 29:**959–977, 1977

34. Majors A, Xue M, Ng TC, et al: Short echo time proton spectroscopy of human brain using a gradient head coil. **Magn Reson Imaging 10:**649–654, 1992
35. Michaelis T, Merboldt KD, Bruhn H, et al: Absolute concentrations of metabolites in the adult human brain *in vivo*: quantification of localized proton MR spectra. **Radiology 187:** 219–227, 1993
36. Michaelis T, Merboldt KD, Hänicke W, et al: On the identification of cerebral metabolites in localized ^{1}H NMR spectra of human brain *in vivo*. **NMR Biomed 4:**90–98, 1991
37. Moonen CTW, von Keinlin M, van Zijl PCM, et al: Comparison of single-shot localization methods (STEAM and PRESS) for *in vivo* proton NMR spectroscopy. **NMR Biomed 2:**201–208, 1989
38. Morantz RA: The management of the patient with low-grade cerebral astrocytomas, in Morantz RA, Walsh JW (eds): **Brain Tumors. A Comprehensive Text.** New York: Marcel-Dekker, 1994, pp 387–415
39. Negendank W, Sauter R, Brown T, et al: Intratumoral lipids and lactate in ^{1}H MRS *in vivo* in astrocytic tumors. **Proc Soc Magn Reson Med 3:**1296, 1994 (Abstract)
40. Negendank W, Zimmerman R, Gotsis E, et al: A cooperative group study of 1H MRS of primary brain tumors. **Proc Soc Magn Reson Med 3:**1521, 1993 (Abstract)
41. Nelson JS, Tsukada Y, Schoenfeld D, et al: Necrosis as a prognostic criterion in malignant supratentorial, astrocytic gliomas. **Cancer 52:**550–554, 1983
42. Ordidge RJ, Cresshull ID: The correction of transient B_o field shifts following the application of pulsed gradients by phase correction in the time domain. **J Magn Reson 69:**151–155, 1986
43. Ott D, Hennig J, Ernst T: Human brain tumors: assessment with *in vivo* proton MR spectroscopy. **Radiology 186:**745–752, 1993
44. Patronas NJ, Di Chiro G, Kufta C, et al: Prediction of survival in glioma patients by means of positron emission tomography. **J Neurosurg 62:**816–822, 1985
45. Peeling J, Sutherland G: High-resolution ^{1}H NMR spectroscopy studies of extracts of human cerebral neoplasms. **Magn Reson Med 24:**123–136, 1992
46. Posse S, Schuknecht B, Smith ME, et al: Short echo time proton MR spectroscopic imaging. **J Comput Assist Tomogr 17:** 1–14, 1993
47. Preul MC, Caramanos Z, Collins JG, et al: Linear discriminant analysis based on proton MR spectroscopic imaging of human brain tumours improves pre-operative diagnosis. **Proc Soc Magn Reson 2:**125, 1994 (Abstract)
48. Radlbauer R, Langenberger KW, Moser E: Qualitätskontrolle für die lokalisierte In-vivo-Protonenspektroskopie an klinischen MR-Geräten. **Roto Fortschr Geb Rontgenstr Neuen Bildgeb Verfahr 160:**254–259, 1994
49. Remy C, Arús C, Ziegler A, et al: *In vivo*, *ex vivo* and *in vitro* one- and two-dimensional nuclear magnetic resonance spectroscopy of an intracerebral glioma in rat brain: assignment of resonances. **J Neurochem 62:**166–179, 1994
50. Russell DS, Rubinstein LJ: **Pathology of Tumors of the Nervous System, ed 4.** Baltimore: Williams & Wilkins, 1977
51. Rutter A, Hugenholtz H, Saunders JK, et al: Classification of brain tumors by ex vivo ^{1}H NMR spectroscopy. **J Neurochem 64:**1655–1661, 1995
52. Salcman M (ed): **Neurobiology of Brain Tumors.** Baltimore: Williams & Wilkins, Vol 4, 1991
53. Sauter R: Cerebral single volume proton spectroscopy on healthy volunteers. A multicenter pilot study. **Proc Soc Magn Reson Med 12:**1531, 1993 (Abstract)
54. Scherer HJ: Cerebral astrocytomas and their derivatives. **Am J Cancer 40:**159–198, 1940
55. Schick F, Nägele T, Klose U, et al: Lactate quantification by means of PRESS spectroscopy—influence of refocusing pulses and timing scheme. **Magn Reson Imaging 13:**309–319, 1995
56. Schifter T, Hoffman JM, Hanson MW, et al: Serial FDG-PET studies in the prediction of survival in patients with primary brain tumors. **J Comput Assist Tomogr 17:**509–516, 1993
57. Segebarth CM, Balériaux DF, Luyten PR, et al: Detection of metabolic heterogeneity of human intracranial tumors *in vivo* by ^{1}H NMR spectroscopic imaging. **Magn Reson Med 13:** 62–76, 1990
58. Sutton LN, Wang Z, Gusnard D, et al: Proton magnetic resonance spectroscopy of pediatric brain tumors. **Neurosurgery 31:**195–202, 1992
59. Sutton LN, Wehrli SL, Gennarelli L, et al: High-resolution ^{1}H-magnetic resonance spectroscopy of pediatric posterior fossa tumors *in vitro*. **J Neurosurg 81:**443–448, 1994
60. Tzika AA, Vigneron DB, Ball WS Jr, et al: Localized proton MR spectroscopy of the brain in children. **J Magn Reson Imaging 3:**719–729, 1993
61. Usenius JPR, Kauppinen RA, Vainio PA, et al: Quantitative metabolite patterns of human brain tumors: detection by ^{1}H NMR spectroscopy *in vivo* and *in vitro*. **J Comput Assist Tomogr 18:**705–713, 1994
62. Winger MJ, Macdonald DR, Cairncross JG: Supratentorial anaplastic gliomas in adults. The prognostic importance of extent of resection and prior low-grade glioma. **J Neurosurg 71:** 487–493, 1989

Manuscript received December 23, 1994.
Accepted in final form August 17, 1995.
Address reprint requests to: William G. Negendank, M.D., Department of NMR and Medical Spectroscopy, Fox Chase Cancer Center, 7701 Burholme Avenue, Philadelphia, Pennsylvania 19111.